Nuclear Inst. and Methods in Physics Research, A 986 (2021) 164808

Contents lists available at ScienceDirect

Nuclear Inst. and Methods in Physics Research, A

journal homepage: www.elsevier.com/locate/nima

Cold neutron radiation dose effects on a ^{6}LiF:ZnS(Ag) neutron detector with wavelength shifting fibers and SiPM photodetector

K. Pritchard [a,*], D. Hussey [b], A. Osovizky [c], J. Ziegler [a], E. Binkley [a], P. Tsai [a], N. Hadad [a], M. Jackson [d], C. Hurlbut [d], G.M. Baltic [a], C.F. Majkrzak [a], N.C. Maliszewskyj [a]

[a] NIST Center for Neutron Research, Gaithersburg, MD, United States of America
[b] NIST Physical Measurement Laboratory, Gaithersburg, MD, United States of America
[c] Rotem Industries Ltd, Rotem Industrial Park, Israel
[d] Eljen Technology, Sweetwater, TX, United States of America

ABSTRACT

A ^{6}LiF:ZnS(Ag) based cold neutron detector with wavelength shifting (WLS) fibers and SiPM photodetector was developed at the NIST Center for Neutron Research for the CANDoR instrument (Chromatic Analysis Neutron Diffractometer or Reflectometer). A series of detectors were irradiated with neutron doses ranging between 1E+11 n/cm^2 to 6E+12 n/cm^2. It was found that the neutron absorbing ^{6}Li isotope was not measurably depleted, but the photonic yield of the detector deteriorated with increasing neutron dose. Photonic yields were compared before and after neutron exposure by comparing pulse energy spectrum photopeaks before and after exposure. A typical detector used in the CANDoR instrument is expected to withstand a cumulative cold neutron dose of at least 1E+12 n/cm^2 before degrading to an unfit state. The component parts of the detector could not be separated, so the degradation of the bulk scintillator and WLS fibers could not be gauged separately.

1. Introduction

Scintillators are materials which convert high energy radiation into a photon signal for X-ray and particle physics applications. High energy radiation energizes the electronic structure of a scintillator as it travels through the material. Photons are released during the process of electron relaxation. A typical commercial scintillator, such as NaI(Tl), yields tens of thousands of photons per 1 MeV of dissipated particle energy. Scintillators may have varying photon production efficiencies for different radiation classes such as photon, alpha, or beta [1–3].

A thermal neutron scintillator combines a standard scintillator material with a neutron absorbing isotope such as lithium-6 or boron-10. Lithium-6 decays following neutron absorption and generates 4.78 MeV of energy via an alpha particle and a triton (tritium nucleus). The decay products dissipate their energy very locally, generally less than a 50 μm path length in solids and liquids [4–7].

The NIST Center for Neutron Research has developed a ^{6}LiF:ZnS(Ag) scintillating neutron detector with wavelength shifting (WLS) fibers [8, 9] for routing light to a silicon photomultiplier (SiPM) [8–11]. The detector diagram and a photograph are shown in Figs. 1 and 2. More information can be found regarding the scintillator composition [10, 11], the design and optimization [12,13], the SiPM [14], and signal processing [15].

The performance of scintillators has been shown to degrade from accumulated radiation damage, as the clarity of the scintillator material lessens. Plastic scintillators have been shown to degrade from gamma exposure [16–18], high energy protons [19], and high energy neutrons [20,20,21]. Inorganic scintillators also show wear after radiation exposures of various types including gammas, high energy protons, and high energy neutrons [22,23]. In addition to just scintillator materials, light guides, optical glues, and wavelength shifters also show radiation damage in a more comprehensive review [24].

Plastic and inorganic scintillators have been studied with high energy radiation, but less research has been done with thermal/cold neutron scintillators using thermal neutrons with non-ionizing energies of 25 meV or less. One study of glass scintillators loaded with ^{6}Li neutron absorber showed no measurable decrease in performance after absorption of 1E+13 cm^{-3} of cold neutrons [25]. Another study showed severe damage to scintillating fibers from a thermal neutron environment, although the environment also contained roughly 2% fast neutrons as well as a significant gamma field which are both capable of ionization [26]. Irradiation of scintillators with purely cold or thermal neutrons has not been widely studied, and so accessing the durability of the CANDOR detector in a cold neutron field was necessary for characterizing the detector's radiation hardness.

2. Optical yield and detection efficiency

Although ZnS(Ag) is a very bright scintillator [7], there are drastic losses to the photon yield before a signal is read out from the SiPM. A

* Corresponding author.
E-mail address: kevin.pritchard@nist.gov (K. Pritchard).

https://doi.org/10.1016/j.nima.2020.164808
Received 21 September 2020; Received in revised form 15 October 2020; Accepted 19 October 2020
Available online 26 October 2020

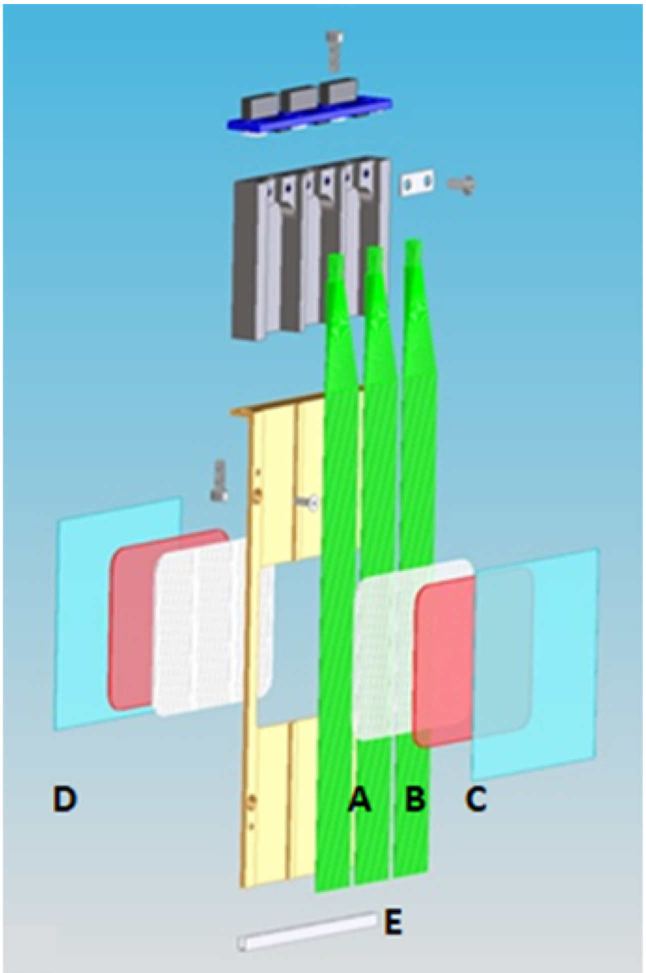

Fig. 1. CAD model of the CANDOR neutron detector. (A, green) wavelength shifting fibers, (B, white) ^{6}LiF:ZnS(Ni) primer layer, (C, pink) ^{6}LiF:ZnS(Ag) scintillator slab, (D, blue) Reflectors, (E) WLS fiber reflector termination.. (For interpretation of the references to color in this figure legend, the reader is referred to the web version of this article.)

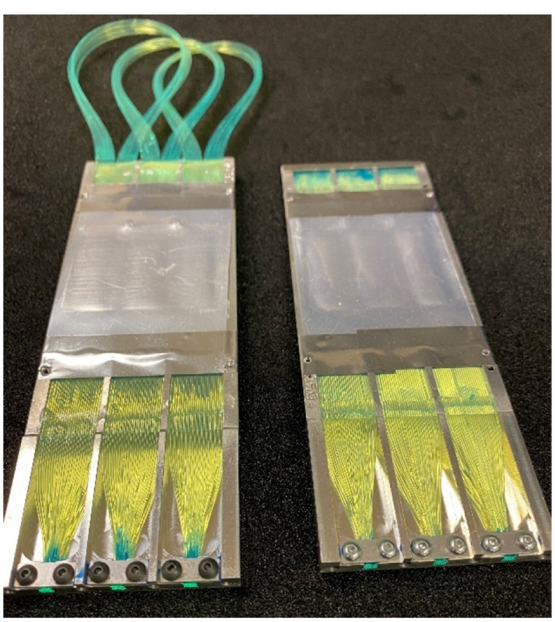

Fig. 2. Photograph of two triple-channel detectors.

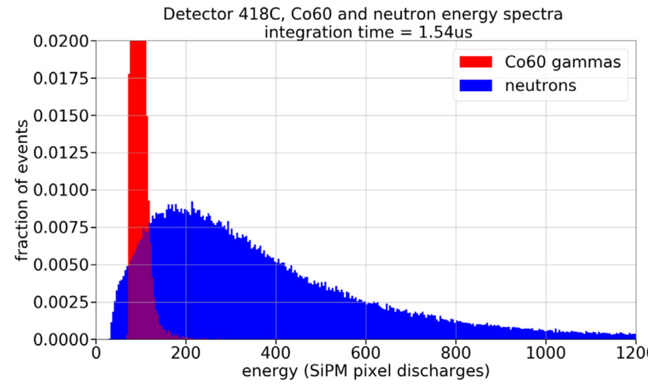

Fig. 3. Pulse Height Distributions (Energy Spectra) of Co-60 gammas and neutrons.

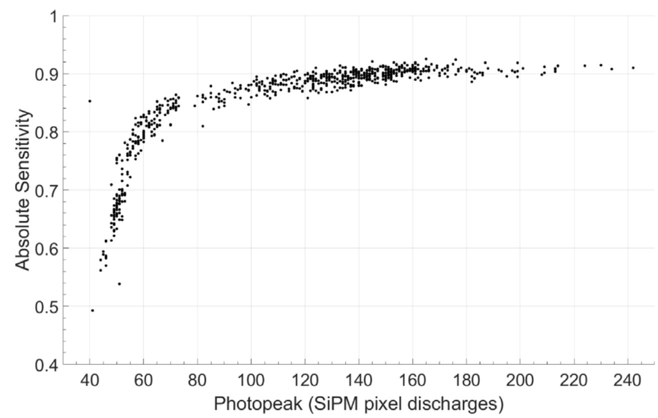

Fig. 4. Absolute sensitivity as a function of photopeak.

typical CANDOR detector has a photopeak between 100–200 SiPM pixel discharges per neutron event. The number of SiPM pixel discharges is closely related to the number of photons incident on the SiPM. Fig. 3 shows a pulse height spectrum normalized to SiPM pixel discharges. The neutron photopeak is fairly broad, centered at about 200 SiPM pixel discharges.

As few as 40 detected photons are sufficient for reliable neutron detection after pulse shape discrimination techniques are used [15]. With a photopeak of 100 or 200 detected photons, the vast majority of neutron events will be identified. To show performance trends, the neutron detection efficiency is mapped as a function of the photopeak in Fig. 4.

A detector with typical performance has a photopeak of 140 pixel discharges, and a detection efficiency of 89% for cold (4.74 Å, 4.9 meV) neutrons. As the optical quality of a detector diminishes down to a photopeak of 80 or 90, the efficiency drops gradually. Below 70, the neutron detection efficiency worsens much more rapidly as photon yield decreases.

An investigation was conducted to see what effects neutron radiation would have on the CANDOR detector. If neutron radiation causes damage to the detector, how severe is the effect? The effects of thermal/cold neutron radiation were investigated exclusively, neglecting gamma dose studies, as cold neutron radiation is by far the most dominant radiation type in situ.

3. Materials and methods

Detectors were measured before and after neutron exposure at the NCNR Multi-Purpose Test Station (PHADES). The PHADES location uses a highly oriented pyrolytic graphite monochromator set at a fixed angle to steer a 4.87 meV (4.1 Å) neutron beam into a shielded cavity formed

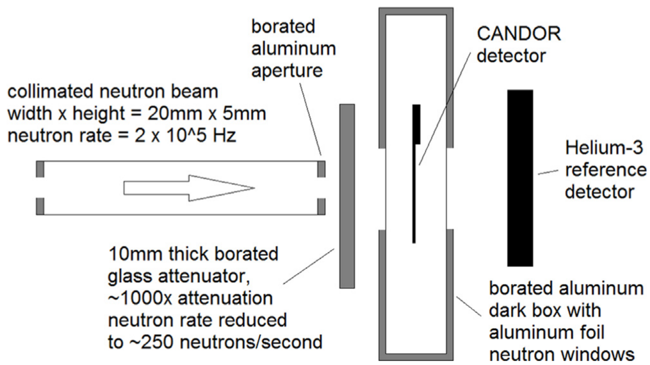

Fig. 5. Detector measurement station diagram.

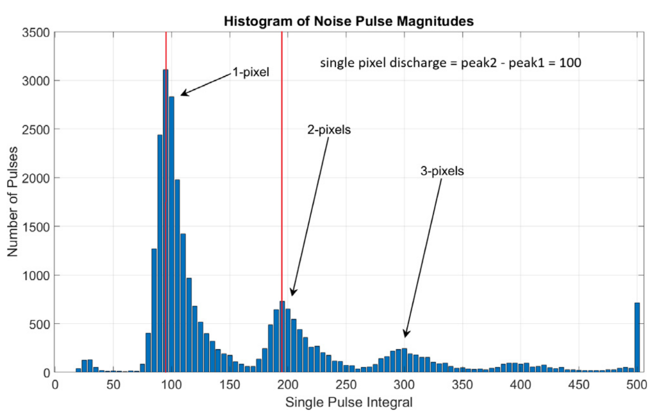

Fig. 6. Histogram of SiPM thermal noise pulses.

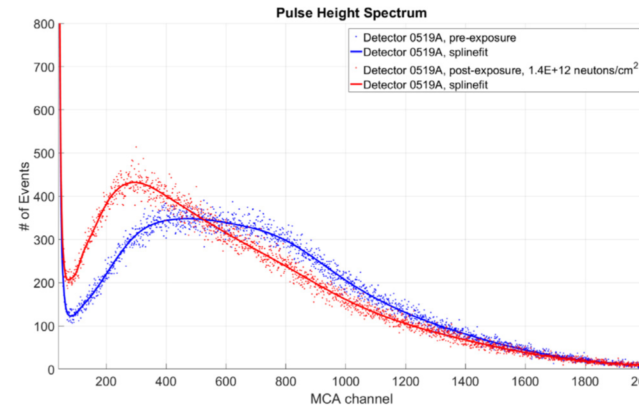

Fig. 7. Pulse height spectra before and after exposure (scale not normalized to SiPM pixel discharges).

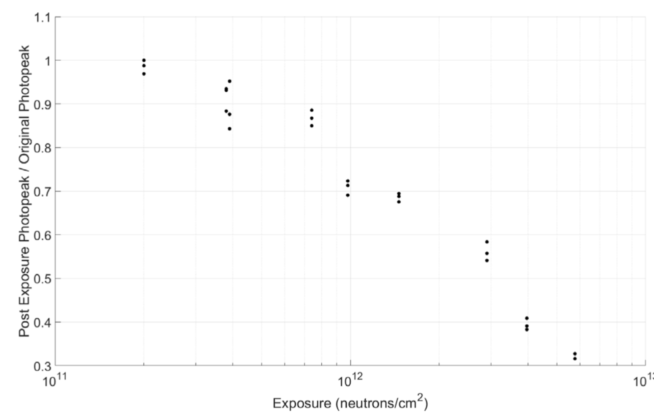

Fig. 8. Post/pre exposure photopeak ratios.

of borated polyethylene. Post-collimation, the rectangular beam had a width of 5 mm, a height of 20 mm, and the beam current can be varied using borated glass attenuators. Our most recent measurements use a beam current of approximately 250 neutrons per second. A diagram illustrates the setup in Fig. 5

Pulse height spectra of each detector were compiled using a XIA PIXIE32 waveform digitizer sampling at 62.5 MSPS, which was programmed to output charge integrals for each event. The charge integration window was from 0 μs to 1.4 μs following the rising edge of a neutron pulse. The charge integrals were normalized to units of SiPM pixel discharges using the average single pixel discharge which was measured from a thermal noise histogram (Fig. 6 and Eq. (1)).

$$single\ pixel\ discharge = x_{peak2} - x_{peak1} \tag{1}$$

To expose detectors to a high flux of cold neutrons, the detectors were placed in the pre-collimated beam at the NG6 neutron imaging station [26]. The beam flux at this location is approximately 2E+9 n/cm^2/s. The detectors were oriented with their front face toward the neutron beam. A progression of 9 exposure times were used to dose 9 different detectors, plus one unexposed detector as a control. The SiPM photodiodes were removed from the assembly prior to the neutron exposures and were not dosed. 9 different detectors were exposed instead of exposing the same detector 9 times and characterizing after each exposure. There were two reasons for this approach. One reason was for quick exposure and testing. Exposing and testing the same detector multiple times would take more coordination and beamtime at the high flux imaging station at NG6. A second benefit of exposing multiple detectors is testing for consistent trends. Trends that pervade 9 different detectors induce to a larger, more diverse population of detectors. A single detector exposed multiple times was not attempted, not even for the purpose of comparing with single-exposed detectors.

To gauge optical degradation, the photopeak was measured before and after exposure, and the post/pre photopeak ratio is used as the metric of optical degradation. An example post/pre pulse height spectrum is shown in Fig. 7. Note that the scale of these pulse height spectra have not been normalized to SiPM pixel discharges, but the post/pre ratio is unaffected. The post/pre ratio in this example is 280/450, or 0.622.

4. Results

The post/pre exposure photopeak ratios were calculated for all 10 detectors and plotted in Fig. 8. The post/pre ratio of the unexposed control detector was 1.024 ± 0.027 (1σ).

Following neutron dose exposures, neutron transmission through the detectors was not measurably affected, implying that the neutron absorbing lithium-6 was not depleted. This was expected as the neutron doses are miniscule compared to the lithium-6 concentration per unit area.

5. Discussion

For the NCNR's purposes, these dose measurements were used to estimate the maximum cumulative exposure for detectors in the CANDOR instrument. Detectors installed in the CANDOR instrument have photopeaks meeting or exceeding 120 SiPM pixel discharges. And so, these detectors can lose 30% or more of their photopeak value before they reach the fitness cutoff of 75 SiPM pixel discharges. This optical loss is not realized until a cumulative dose of 10E+12 n/cm^2 has been reached. In a typical use case at CANDOR, this exposure limit would not be reached for decades, since the neutron intensity on a detector averages less than 1000 n/cm^2/s. However, the shelf-life of these detectors has not been studied extensively. Early prototype detectors which were resting on a shelf at room temperature and humidity for 2 years were re-tested with no noticeable change in performance, but a systematic shelf-life study was not performed. For a comprehensive longevity study, detectors in the CANDOR instrument will be monitored periodically over time.

It is unclear whether most of the optical damage is found in the LiF:ZnS(Ag) scintillator or in the WLS fibers, as the two components are not separable. After removing the surface reflectors, there was some discoloration to the front face of the LiF:ZnS(Ag) bulk scintillator. The WLS fibers could not be examined. It is logical that most degradation would be located in the bulk scintillator material rather than in the WLS fibers, because the high energy decay products are produced within the bulk scintillator and have short pathlengths of approximately 30 μm – 40 μm. Only a small percentage of these decay products would escape the bulk scintillator to interact with the outer cladding layer of the WLS fibers.

6. Conclusion

Radiation hardness of a LiF:ZnS(Ag) cold neutron detector was tested. Detectors were irradiated with cold neutron doses ranging from 2E+11 n/cm^2 to 6E+12 n/cm^2. Detector characteristics such as neutron absorption and optical yield were measured before and after neutron exposures and compared. It was found that the neutron absorption of the detectors was not affected in a measurable way, and the optical yield decreased with additional neutron exposure. The component materials of the detectors could not be separately tested, and so damage was not separately gauged in the bulk scintillator and WLS fibers, although discoloration to the bulk scintillator post-exposure was observed. The results of these tests suggest that detectors installed in the CANDOR instrument are able to withstand a cold neutron dose up to 1E+12 n/cm^2 before degrading to an unfit state.

Disclaimer

Certain commercial equipment, instruments, or materials (or suppliers, or software, …) are identified in this paper to foster understanding. Such identification does not imply recommendation or endorsement by the National Institute of Standards and Technology, nor does it imply that the materials or equipment identified are necessarily the best available for the purpose. This work benefitted from the Center for Neutron Research at the National Institute of Standards and Technology; this facility is funded by the U.S. Department of Commerce.

CRediT authorship contribution statement

K. Pritchard: Methodology, Formal analysis, Investigation, Writing. **D. Hussey:** Resources, Supervision. **A. Osovizky:** Supervision. **J. Ziegler:** Resources. **E. Binkley:** Resources. **P. Tsai:** Resources. **N. Hadad:** Project administration. **M. Jackson:** Resources. **C. Hurlbut:** Resources. **G.M. Baltic:** Funding acquisition. **C.F. Majkrzak:** Supervision, Conceptualization. **N.C. Maliszewskyj:** Supervision, Conceptualization.

Declaration of competing interest

The authors declare that they have no known competing financial interests or personal relationships that could have appeared to influence the work reported in this paper.

References

[1] G. Knoll, Radiation Detection and Measurement, fourth ed., John Wiley & Sons, Inc., United States, 2010.

[2] S. Derenzo, M. Boswell, M. Weber, K. Brennan, Scintillation Properties, Lawrence Berkeley National Laboratory.

[3] R. Hofstadter, Alkali halide scintillation counters, Phys. Rev. 74 (100) (1948) http://dx.doi.org/10.1103/PhysRev.74.100.

[4] V.S. Litvin, A.D. Beyaev, S.M. Ignatov, V.S. Litvin, A.D. Beyaev, S.M. Ignatov, ZnS(Ag)/6LiF and LiI(Eu) scintillaotrs and silicon photomultipliers for thermal neutron detetctors with high space and time resolution, Bull. Russ. Acad. Sci. Phys. 73 (2009) 219–221.

[5] C.W.E. Eijk, Inorganic scintillator development, Nucl. Instrum. Methods Phys. Res. A 460 (2001) 1–14.

[6] C.W.E. van Eijk, Inorganic scintillators for thermal neutron detection, IEEE Trans. Nucl. Sci. 59 (5) (2012) 2242–2247, http://dx.doi.org/10.1109/TNS.2012.2186154.

[7] A. Tsunesaburo, M. Masayoshi, O. Masayuki, Decay properties of ZnS(Ag) phosphors, J. Phys. Soc. Japan 14 (12) (1959) 1766–1770.

[8] Wavelength Shifting Fibers. Kuraray Co. Ltd.

[9] Plastic Scintillating Fibers (Materials and Structures). Kuraray Co. Ltd.

[10] Y. Yehuda-Zada, et al., Optimization of 6LiF:ZnS(Ag) Scintillator Light Yield using GEANT4, 2018.

[11] A. Osovizky, et al., 6LiF:ZnS(Ag) Mixture Optimization for a Highly Efficient Ultrathin Cold Neutron Detector, 2018.

[12] N.C. Maliszewskyj, et al., An energy analyzing detector for cold neutrons, 2018.

[13] A. Osovizky, et al., Design of an Ultrathin Cold Neutron Detector, 2018.

[14] A. Osovizky, et al., Selection of silicon photomultipliers for a 6LiF:ZnS(Ag) scintillator based neutron detector, 2018.

[15] K. Pritchard, et al., Computational techniques for optimizing a 6LiF:ZnS(Ag) neutron detector using recorded waveforms, 2019.

[16] CMS Collaboration, Measurements of dose-rate effects in the radiation damage of plastic scintillator tiles using silicon photomultipliers, 2020, arXiv:2001.06553 Hep-Ex Physicsphysics.

[17] S.V. Afanasiev, et al., Light yield measurements of 'finger' structured and unstructured scintillators after gamma and neutron irradiation, Nucl. Instrum. Methods Phys. Res. A 818 (2016) 26–31, http://dx.doi.org/10.1016/j.nima.2016.02.045.

[18] S. Baccaro, et al., Radiation damage tests on diamond and scintillation detector components for the ITER radial neutron camera, IEEE Trans. Nucl. Sci. 65 (8) (2018) 2046–2053, http://dx.doi.org/10.1109/TNS.2018.2807841.

[19] H. Jivan, J.E. Mdhluli, E. Sideras-Haddad, B. Mellado, R. Erasmus, M. Madhuku, Radiation damage effects on the optical properties of plastic scintillators, Nucl. Instrum. Methods Phys. Res. B 409 (2017) 224–228, http://dx.doi.org/10.1016/j.nimb.2017.05.061.

[20] J.E. Mdhluli, et al., Neutron induced radiation damage of plastic scintillators for the upgrade of the Tile Calorimeter of the ATLAS detector, J. Phys. Conf. Ser. 878 (2017) 012008, http://dx.doi.org/10.1088/1742-6596/878/1/012008.

[21] V. Baranov, et al., Effects of neutron radiation on the optical and structural properties of blue and green emitting plastic scintillators, Nucl. Instrum. Methods Phys. Res. B 436 (2018) 236–243, http://dx.doi.org/10.1016/j.nimb.2018.10.002.

[22] C. Hu, et al., Neutron-induced radiation damage in BaF_2, LYSO/LFS and PWO crystals, J. Phys. Conf. Ser. 1162 (2019) 012020, http://dx.doi.org/10.1088/1742-6596/1162/1/012020.

[23] C. Hu, et al., Proton-induced radiation damage in BaF_2, LYSO, and PWO crystal scintillators, IEEE Trans. Nucl. Sci. 65 (4) (2018) 1018–1024, http://dx.doi.org/10.1109/TNS.2018.2808841.

[24] Yu.N. Kharzheev, Radiation hardness of scintillation detectors based on organic plastic scintillators and optical fibers, Phys. Part. Nucl. 50 (1) (2019) 42–76, http://dx.doi.org/10.1134/S1063779619010027.

[25] G. Ban, et al., First tests of Li-6 doped glass scintillators for ultracold neutron detection, J. Res. Natl. Inst. Stand. Technol. 110 (3) (2005) 283, http://dx.doi.org/10.6028/jres.110.040.

[26] D.S. Hussey, et al., A new cold neutron imaging instrument at NIST, Phys. Proc. 69 (2015) 48–54, http://dx.doi.org/10.1016/j.phpro.2015.07.006.